ACS Catalysis

Research Article

pubs.acs.org/acscatalysis

Coverage-Induced Conformational Effects on Activity and Selectivity: Hydrogenation and Decarbonylation of Furfural on Pd(111)

Shengguang Wang, Vassili Vorotnikov, and Dionisios G. Vlachos*

Department of Chemical and Biomolecular Engineering, Catalysis Center for Energy Innovation, and Center for Catalytic Science and Technology, University of Delaware, Newark, Delaware 19716, United States

Supporting Information

ABSTRACT: Adsorption, hydrogenation, and decarbonylation of furfural on hydrogen-covered Pd(111) was investigated using density functional theory calculations. It was found that both the energy and the conformation of adsorbed furfural vary with increasing coverage of hydrogen or furfural. Furfural lies flat at low coverage but becomes tilted on crowded surfaces. The energy profiles of hydrogenation and decarbonylation reactions on a hydrogen-covered Pd(111) change profoundly compared to those on bare Pd(111). The energy span theory shows that the furfural hydrogenation and decarbonylation effective barriers exhibit a maximum with increasing hydrogen coverage. In contrast, the selectivity to hydrogenation toward furfuryl alcohol over decarbonylation is favored with increasing hydrogen coverage. Microkinetic modeling suggests that the conformation change with increasing H coverage has a significant effect on reaction rates (up to orders of magnitude) and induces a selectivity reversal from furan as the main product (low-H coverage limit) to furfuryl alcohol (high-H coverage limit). Our results may rationalize different selectivity trends seen experimentally under typical reactor and UHV conditions. Importantly, this study underscores the potential importance of operating conditions on hydrodeoxygenation activity and selectivity due to conformational changes of multifunctional biomass derivatives.

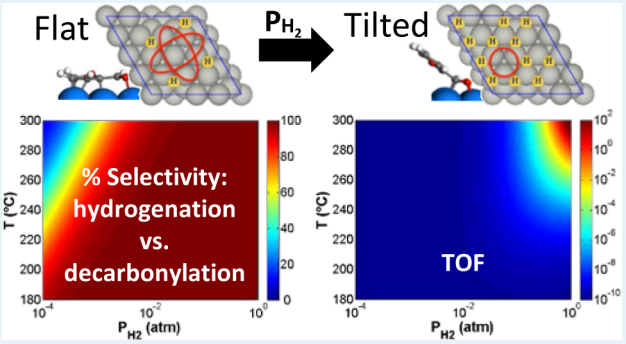

KEYWORDS: *furfural, furfuryl alcohol, furan, Pd, hydrogenation, decarbonylation, coverage effects, conformation effect*

INTRODUCTION

Furfural is one of the important intermediates in the production of biofuels.[1] Furfural is directly obtained by the acid-catalyzed dehydration of xylose, the main building block of hemicellulose, one of the key biomass constituents. Due to its high reactivity, furfural requires further upgrade to more stable products in order to incorporate them to the gasoline/diesel pool or use them as chemicals (e.g., the production of aromatics, such as toluene).[2] Mild hydrogenation, without furan ring hydrogenation, is one such potential upgrade route.

It is important to find effective hydrogenation catalysts and identify the reaction pathways.[3] Recent research has shown that different metals exhibit different product distributions. For example, Cu-based catalysts are highly selective for hydrogenation of furfural to furfuryl alcohol (>95% selectivity).[4] In contrast, Group VIII metals (Ni, Pd, and Pt) at low temperatures exhibit mainly hydrogenation activity, with furfuryl alcohol as the major product[5−7] at high temperatures, the decarbonylation reaction dominates, with furan being the main product.[8]

In the past, density functional theory (DFT) calculations and experiments have been conducted to investigate the nature of the adsorbed species.[9−15] DFT calculations showed that the adsorption of furfural on Cu results in an η^1(O)−surface species, in which the carbonyl group is bound to the metal through the O lone pair, whereas the rest of the molecule is away from the surface due to a net repulsion between C and Cu. The preferred η^1(O)−adsorption mode has been proposed as the reason for the high hydrogenation selectivity to furfuryl alcohol, typically observed on Cu-based catalysts.[9−11] Greeley and co-workers studied the hydrogenation of furfural to furfuryl alcohol on Pd(111), Cu(111), and Pt(111) using DFT calculations. The adsorbed structures were found to be flat on Pd(111) and Pt(111) and tilted on Cu(111).[12] Other groups have also found different adsorption geometries of furfural on Cu and Pd; the differences in selectivities seen experimentally were generally attributed to differences in conformation.[4,13,14]

Even though there are a few adsorption DFT studies of furans on metal surfaces, comprehensive computational kinetic studies are very limited. Our group has calculated the thermodynamics and kinetic barriers of furfural conversion to furan, furfuryl alcohol, and 2-methylfuran on Pd(111), using dispersion-corrected DFT calculations, and found that the most stable conformation for furan, furfural, furfuryl alcohol, and 2-methylfuran entails the furan ring lying flat on the surface,

Received: October 2, 2014
Revised: November 13, 2014
Published: November 14, 2014

centered over a hollow site.[15] In addition, we have extended these studies to ring opening and ring hydrogenation.[16]

The above computational studies have been conducted at the low coverage limit. Experimentally, the coverage is often not known. Recently Medlin and co-workers introduced an elegant method of restricting the flat adsorption geometry on Pd terrace sites and by doing so increased the selectivity to furfuryl alcohol and methylfuran.[17] Clearly, exogenous control of conformation can have a major impact on selectivity. Because operating conditions can significantly vary coverages (endogenous control), the study of Medlin and co-workers begs the question of how the coverage affects activity and selectivity.

Medlin and co-workers reviewed the effects of adsorbate−adsorbate interactions in other reaction systems, such as the hydrogenation of olefins with other carbonaceous adsorbates present, and the coadsorption of alkalis, halides, and other inorganic "poisons" to improve selectivity.[18] Other researchers also found that adsorbate−adsorbate interactions can have profound effects on catalyst activity.[19−23] Medlin and co-workers' DFT and HREELS results indicated that the coverage dependence of the reaction pathways correlates with a change in the adsorption geometry of hydroxyethyl.[24] The extent to which adsorbate−adsorbate interactions can affect selectivity remains an open question; no prior theoretical calculations have addressed this question for multifunctional biomass derivatives.

In this paper, we investigate the effect of adsorbate−adsorbate interactions on furfural adsorption and furfural hydrogenation to furfuryl alcohol and decarbonylation to furan using DFT calculations along with simple kinetic and microkinetic analyses. The reactions considered are shown in Scheme 1. The effects of pressure and temperature are also discussed. We demonstrate one of the first examples of coverage-induced selectivity reversal.

Scheme 1. Reaction Scheme of Furfural Hydrogenation and Decarbonylation on H-Precovered Pd(111) Surface

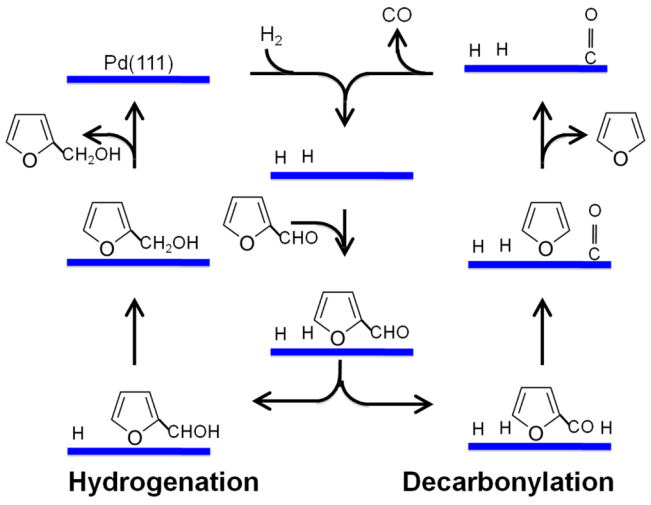

METHODS AND MODELS

DFT Methods. We carried out plane-wave DFT calculations using the Vienna ab initio simulation package (VASP), version 5.2.12.[25,26] The electron−electron exchange and correlation energies were computed using the Perdew, Burke, and Ernzerhof functional with the latest dispersion correction, PBE−D3.[27,28] Our previous work has shown that the PBE-D3 produces more reasonable binding energies for furan compounds.[15] The projector augmented-wave method was used for the electron−ion interactions.[29,30] We used a plane-wave basis set with an energy cutoff of 400 eV.

For bulk calculations, a tetrahedron method with Blochl corrections and 15 × 15 × 15 Monkhorst−Pack k-point mesh was used.[31,32] The bulk lattice constant was obtained using the Birch−Murnaghan equation of state. The Pd fcc lattice constant, calculated to be 3.90 Å using PBE−D3, is in good agreement with the experimental value of 3.89 Å.[33] The supercell for all gas-phase calculations was chosen to be 20 × 20 × 20 Å.

The metal slab was modeled with a 4 × 4 unit cell composed of four atomic layers. The bottom two layers were frozen. The vacuum between the slabs was set at 20 Å to minimize the effect of the interaction between them. The Brillouin zone was sampled with a 3 × 3 × 1 k−point grid. For accurate total energies, we used the Methfessel−Paxton method with a smearing parameter of 0.1. Surface relaxation was performed until all forces were smaller than 0.05 eV/Å. The transition states were located using the climbing nudged elastic band (cNEB) method.[34] The transition states were confirmed with the presence of a unique imaginary frequency.

The adsorption energy was calculated as $E_{ads} = E_{slab+i} - E_{slab} - E_i$, where E_{slab+i} is the total electronic energy of the adsorbate/slab system, E_{slab} is the total electronic energy of a clean slab, and E_i is the total electronic energy of the adsorbate in the gas phase. The average adsorption energy of n adsorbates on a slab was calculated as $E_{ads} = (E_{ni/slab} - E_{slab} - nE_i)/n$; where $E_{ni/slab}$, E_{slab}, and E_i are the total electronic energies of adsorbate/slab system, clean slab, and adsorbate in gas phase, respectively.

Below we report coverages in monolayers (ML) with respect to the maximum number of each species that can be accommodated on the 4 × 4 Pd surface atoms. The maximum number for furfural is 4 (this is in the tilted conformation but is used in reporting all results; it is only 3 in the flat conformation). For H, we use 16 as the maximum number due to stronger repulsive interaction between the adsorbed hydrogen atoms with more hydrogens on the slab.

Microkinetic Model. In order to explore the ramifications of H coverage on the kinetics, we consider a skeleton microkinetic model consisting of the elementary reactions shown in Table 1. The reaction rate constant parameter estimation methodology has recently been reviewed.[35] The Gibbs free energy of each species is computed using Chemkin with appropriate NASA polynomials developed to determine the heat of formation H_{f298}, the entropy of formation S_{298}, and the specific heat $C_p(T)$ for each gas-phase and each surface species. The gas-phase thermochemistry for H_2, CO, furfural, furfuryl alcohol, and furan was estimated using G4-level ab initio calculations as previously reported.[36] Surface thermochemistry was estimated using a combination of statistical mechanics and first-principles semiempirical correlations. The vibrational frequencies were only computed for the adsorbed furfural, H, and CO, and employed to give statistical mechanics' estimates of H_{f298}, S_{298} and $C_p(T)$ of these surface species. We estimated H_{f298} for the rest of the surface species from the H_{f298} of furfural and the coverage-specific average adsorption energies of atomic hydrogen under the assumption that $\Delta H_{rnx} = \Delta E_{rnx,OK}$. For instance, H_{f298} of FCHOH at 0.5 ML H coverage was estimated from that of FCHO and reaction 1 in Table 1 as

dx.doi.org/10.1021/cs5015145 | ACS Catal. 2015, 5, 104−112

Table 1. Elementary Reactions, DFT-Calculated Reaction Energies ΔE_{rxn}, and Activation Energies E_a at Different Coverages (in eV)[a]

		ΔE_{rxn} at specified H coverages			E_a at specified H coverages		
	reaction	low	0.5 ML	0.75 ML	low	0.5 ML	0.75 ML
	bond scission and formation						
1	FCHO + H = FCHOH	0.41	−0.10	0.41	0.63	0.61	0.61
2	FCHOH + H = FCH_2OH	0.15	0.29	−0.26	0.72	0.88	0.57
3	FCHO = FCO+H	0.09	−0.25	0.14	0.76	0.63	0.94
4	FCO + H = FH+CO	−1.56	−1.08	−0.87	0.62	0.50	0.50
	adsorption/desorption						
5	$1/2H_2(g)$ = H	−0.67	−0.64	−0.62			
6	CO(g) = CO	−2.98	−2.98	−2.98			
7	FCHO(g) = FCHO	−1.96	−1.03	−1.00			
8	$FCH_2OH(g)$ = FCH_2OH	−2.05	−1.43	−1.40			
9	FH(g) = FH	−1.73	−0.66	−0.03			

[a]The values of E_a of reaction 4 at high coverages (last two columns) are estimated using the C−C scission BEP (see text and SI for details).

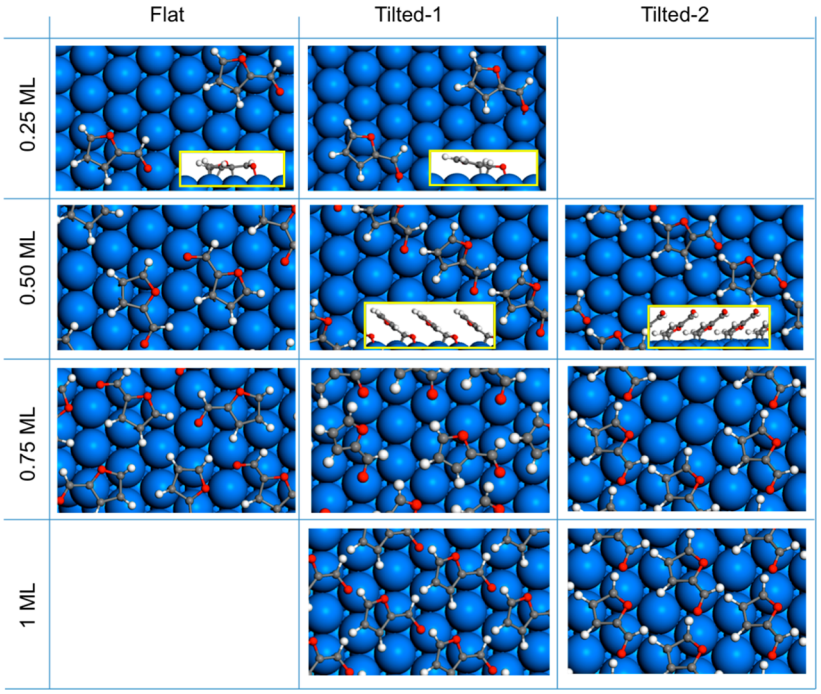

Figure 1. Typical adsorbed structures of furfural on Pd(111) at coverages of 0.25, 0.5, 0.75, and 1 ML. Blank spaces indicate that we were not able to locate stable conformations at this coverage.

shown below. S_{298} and $C_p(T)$ for these species were estimated using group additivity developed for furanic compounds on Pd(111).[36]

$$H_{f298}^{FCHOH} = \Delta E_{FCHO+H\leftrightarrow FCHOH} + H_{f298}^{FCHO} + H_{f298}^{H}$$
$$= -0.10 + (-2.69) + (-0.62) = -3.41\text{eV}$$

DFT-estimated reaction and activation energies are shown in Table 1 for three sets of calculations: (1) low-coverage, taken from our previous work,[15] (2) 0.5 ML of hydrogen, and (3) 0.75 ML of hydrogen and are discussed in the results section. The C−C bond breaking in the acyl intermediate was not considered to be a rate-determining step due to being highly exothermic. For this reason, we have combined the C−C bond breaking and the subsequent furyl hydrogenation to furan in a single reaction step (FCO + H = FH + CO) and estimated its barrier using the C−C scission BEP relation.[43] The BEP predicted a negative barrier, which resulted in an arbitrary choice for this barrier at 0.5 eV. Lower values of this barrier did not affect the results.

In the microkinetic model, the rate constant was computed using transition state theory as shown in eq 1. Because vibrational frequencies were not computed in the high-coverage limits, the entropic contribution to the pre-exponential factor was ignored and the pre-exponential was simply taken to be (k_BT/h), a common assumption in approximate microkinetic modeling.[37] By doing so, we assumed that the activation energies do not vary with temperature over the narrow range considered in this work.

$$k = \frac{k_BT}{h}\exp\left(-\frac{\Delta G^{\ddagger}}{RT}\right) = \frac{k_BT}{h}\exp\left(\frac{\Delta S^{\ddagger}}{R}\right)\exp\left(-\frac{E_a}{RT}\right) \sim \frac{k_BT}{h}\exp\left(-\frac{E_a}{RT}\right) \quad (1)$$

dx.doi.org/10.1021/cs5015145 | ACS Catal. 2015, 5, 104−112

Adsorption was modeled using collision theory with sticking coefficients for H_2, CO, and furanics of 0.1, 0.8, and 1, respectively. The sticking coefficients for H_2 and CO were taken to be the same as the ones for Pt(111).[38] The values of the lateral interactions in the adsorption energy of hydrogen (ΔE_H), CO (ΔE_{CO}), and furanic intermediates (ΔE_F) are 2, 30, and 9 kcal/mol/ML, respectively. The interactions for hydrogen and CO were estimated using DFT calculations, while the ones for furanic intermediates were assumed to be the same as those for furfural on Pd(111).[15] The coverage θ_F was taken as the sum of all individual coverages of furanic intermediates, namely, FCHO, FCHOH, FCH_2OH, FCO, and FH. The positive slopes indicate repulsive interactions (i.e., the adsorption energy becomes less negative with increasing coverage).

We have chosen reactor parameters to reflect those of the experimental work of Resasco and co-workers.[39] We use 95 mol % unreactive diluent, a volumetric flow rate of 8.257 cm^3/s, a surface area to volume ratio of 738 cm^{-1}, a reactor length of 2 cm, and a reactor diameter of 4 mm. Below, we report initial rates and selectivities (entrance rates). The numerical implementation is described elsewhere.[37]

COVERAGE EFFECTS ON ADSORPTION AND FURFURAL CONFORMATION

Effect of Furfural Coverage on its Adsorption. There are four typical adsorbate conformations: the flat, two types of tilted, and the vertical. Figure 1 shows the most stable flat and tilted conformations, among various tested, at different coverages; the average adsorption energies are shown in Figure 2. Our calculations, consistent with prior work on Pd,[15] show that the vertical conformation is not the most stable one on Pd(111), given the very weak adsorption energy (Supporting Information, Figure S1).

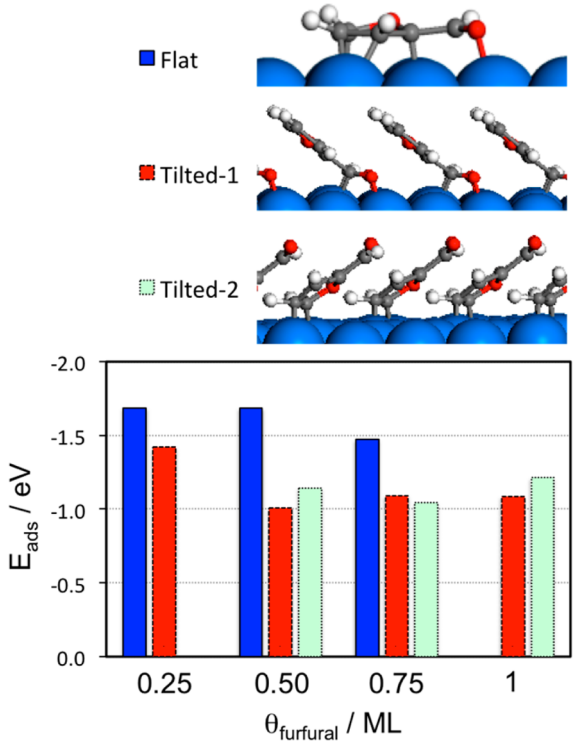

Figure 2. Adsorption energies of the most stable furfural structures on Pd(111) at various coverages of furfural indicated. Tilted-1 binds to Pd(111) mainly via the −CHO group, whereas Tilted-2 binds to Pd(111) via two furan-ring carbons.

The flat conformation of furfural interacts with Pd(111) with both its ring and the carbonyl group. There are two tilted conformations: one in which the two carbons of the furan ring bind to Pd(111) and the −CHO group is slightly tilted away from the surface (Tilted-2) and another in which the −CHO group and a carbon atom of the furan ring bind to the Pd(111) and the furan ring is slightly tilted away from the surface (Tilted-1; hereafter, we refer to Tilted-1 when Pd interacts mainly with the formyl group irrespective of the position of the furan ring). This structure was not stable at lower coverages (0.25 ML).

The adsorption energy of the flat conformation of furfural is nearly unchanged (−1.7 eV) with increasing coverage and decreases only slightly to −1.5 eV when the coverage reaches 0.75 ML. At low coverages, the flat conformation is the most stable due to maximizing the number of bonds with the surface and the strong dispersion forces. At high coverages, the flat conformation is not feasible because of surface crowdedness (i.e., due to packing effects). Instead, the tilted conformations and, in particular, Tilted-2, become the most stable.

For Tilted-1 (red bars in Figure 2), the average adsorption energy drops by 0.4 eV when the coverage increases from 0.25 to 0.5 ML or higher because of the large change in the angle between the furan ring and the surface (Figure 1). At low coverages, binding occurs via the carbon and oxygen atoms of the −CHO group and a furan ring-carbon, with a small angle between the furan ring and Pd(111) surface that facilitates strong van der Waals interactions; at higher coverages, furfural binds to Pd(111) only via the −CHO group, and the angle between the furan ring and Pd(111) surface is larger, leading to weak van der Waals interactions. For the Tilted-2 conformation (green bars in Figure 2), the furan/surface angle is large for all coverages for which this conformation is observed, and as a result, the effect of lateral interactions is small.

In summary, furfural adsorbs flat on Pd(111); the tilted conformation (binding via −CHO or via the ring) becomes favorable with increased crowdedness on the surface. The vertical conformation is not competitive compared to tilted and flat conformations.

Furfural Adsorption on H-Covered Catalyst. Hydrogen is one of the coreactants in furfural hydrogenation. We calculated coverage effects on the adsorption of hydrogen (Supporting Information, Figures S2−S3). The calculated adsorption energy of H at low coverages is −0.67 eV, consistent with literature.[15] With increasing coverage, the adsorption energy decreases slightly up to a coverage of 1 ML. For higher coverages, the adsorption energy drops significantly due to strong repulsive interactions.

Figure 3 shows the structures and adsorption energies of furfural at various coverages of H. We start with θ_H = 0.25 ML. For the flat conformation (Figure 3a), there are two adsorbed hydrogen atoms very close to furfural. The adsorption energy of furfural is much lower than that on bare Pd(111) (−1.04 vs −1.69 eV). For tilted conformations, the most stable one (Figure 3c) binds to Pd(111) with the −CHO group. The adsorption energy of furfural is −0.96 eV, which is lower than that of tilted furfural on bare Pd(111) at 0.25 ML (−1.42 eV). The drop in adsorption energy of the tilted conformation caused by the coadsorbed hydrogen is lower than that of the flat conformation (0.46 vs 0.65 eV). This is in line with the fact

dx.doi.org/10.1021/cs5015145 | ACS Catal. 2015, 5, 104−112

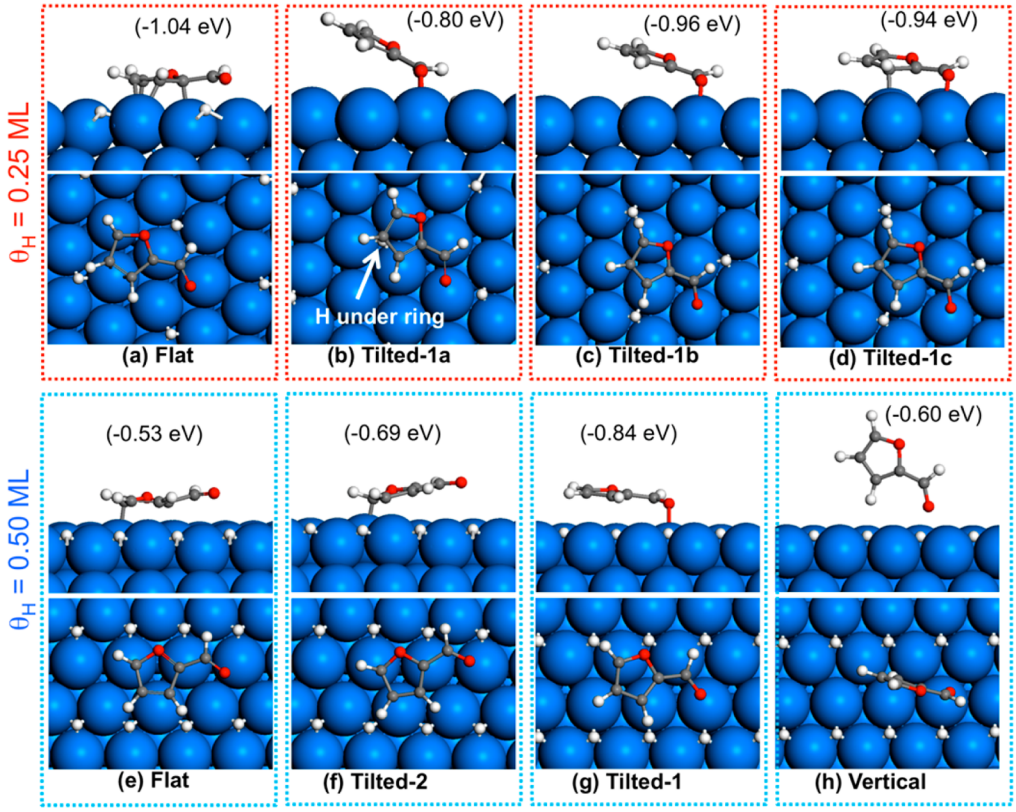

Figure 3. Adsorption structure and energy of furfural at two hydrogen coverages on Pd(111).

that the flat conformation needs more surface area and the surface is more crowded.

The structures and adsorption energies of the Tilted-1a (Figure 3b) and Tilted-1b (Figure 3c) are similar. There is a hydrogen atom located under the furan ring for Tilted-1a, which minimizes the van der Waals interaction of the furan ring with Pd(111). The van der Waals interaction in Tilted-1b structure induces stronger adsorption energy and a smaller angle between the furan ring and Pd(111). Vertical conformations of furfural were not calculated for the H covered Pd(111), because they are not competitive due to their low adsorption energies (−0.66 and −0.69 eV in Figure S1) obtained on bare Pd(111).

Figure 3 also shows the structures and adsorption energies of the adsorbed furfural at θ_H = 0.5 ML. The flat conformation of furfural (Figure 3e) has a significantly lower adsorption energy compared to that of furfural at θ_H = 0.25 ML (−0.53 vs −1.04 eV). Slight rotation of furfural on the surface induces tilting of the molecule (Figure 3f), and the adsorption is stronger than that of the flat conformation (−0.69 vs −0.53 eV) (Figure 3e). However, the most stable tilted conformation (Figure 3g, Tilted-1) has an adsorption energy of −0.84 eV and only the oxygen atom of the −CHO group is close to Pd(111). The majority of the adsorption energy arises from van der Waals interactions between the furfural and the surface. The vertical conformation (Figure 3h) is the least stable conformation. Even at higher coverage of hydrogen of θ_H = 0.75 ML, the tilted conformation is the most stable (adsorption energy is −0.84 eV).

Figure 4 summarizes the adsorption of furfural at various coverages of hydrogen. Furfural binds strongly on bare Pd(111) and the adsorption strength decreases with increasing coverage of hydrogen. An increase in the hydrogen coverage induces a

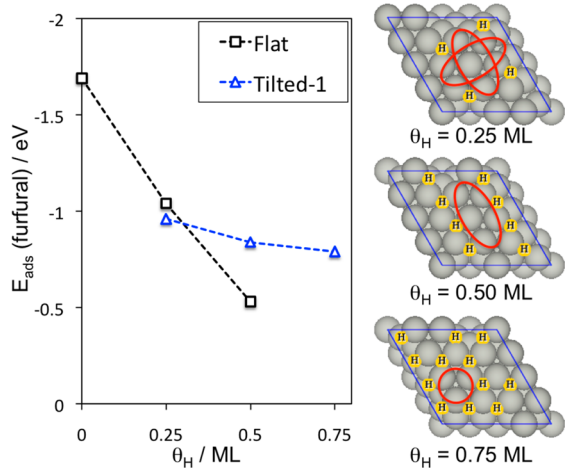

Figure 4. Effect of hydrogen coverage on the adsorption energies of flat and Tilted-1 conformations on Pd(111). Red circles indicate the size of available adsorption areas on select structures of adsorbed H.

conformational change of furfural from flat at low coverages to tilted at higher coverages. This transition occurs at H coverage of $\theta_H \sim$ 0.50 ML. Given the fact that furfural and hydrogen repel each other, we expect that at moderate hydrogen coverages, diffusion of hydrogen farther away from furfural could minimize the free energy and increase the adsorption strength of furfural. In addition, it is well-known that H diffuses into the bulk of Pd crystal. Consequently, the exact coverage of hydrogen where the conformational change happens will be somewhat different from the DFT-estimated value. Nevertheless, the qualitative picture of conformational effects would not change.

dx.doi.org/10.1021/cs5015145 | ACS Catal. 2015, 5, 104−112

FURFURAL HYDROGENATION

Next we turn to understanding the effect of hydrogen coverage on the hydrogenation reaction of furfural, denoted as FCHO. It has been proposed[40] that the first step of furfural hydrogenation is the formation of a C−H bond, yielding an alkoxide intermediate, which is then followed by the addition of the second H atom to this intermediate, forming an adsorbed alcohol. Alternatively, it is also possible that the first step might involve the addition of H to the O atom, thus forming a hydroxylalkyl intermediate, which upon further hydrogenation yields the adsorbed alcohol.

Figure 5 shows the structures and energy barriers of furfural hydrogenation to furfuryl alcohol at θ_H = 0.50 ML. The first

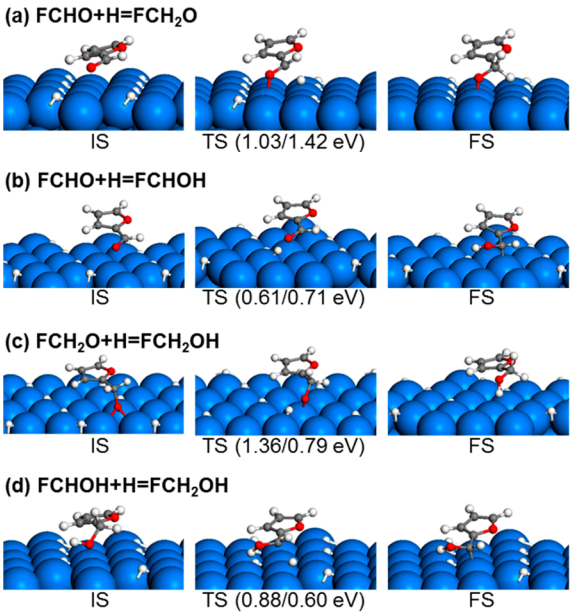

Figure 5. Structures of furfural hydrogenation initial states (IS), transition states (TS), and final states (FS) at 0.5 ML hydrogen coverage on Pd(111). The energies in parentheses are forward and reverse activation energies. Conformations of the intermediates directly connect the transition states and may not be the most stable structures.

hydrogenation of FCHO to FCH_2O (FCHOH) has a reaction barrier of 1.03 eV (0.61 eV). The big difference in energy barriers indicates that the formation of FCHOH intermediate is kinetically likely. The energy barrier of FCH_2O hydrogenation to FCH_2OH is high (1.36 eV), whereas the hydrogenation barrier of FCHOH is lower (0.88). Comparison of the two pathways (1) FCHO+2H → FCH_2O+H → FCH_2OH and (2) FCHO + 2H → FCHOH+H → FCH_2OH (energy profiles in Figure S6), indicates that the hydrogenation reaction via the FCHOH intermediate is kinetically preferred on hydrogen covered Pd(111). This pathway was found to be dominant on bare (no adsorbed H) Pd(111) as well.[15]

We also calculated the structures of the intermediates and transition states along the dominant hydrogenation pathway at θ_H = 0.75 ML (Supporting Information, Figure S7). At this higher H coverage, the forward energy barriers of the first and second hydrogenation steps are comparable to those at θ_H = 0.5 ML. In contrast, the backward reaction of the first hydrogenation step (FCHO+H═FCHOH) has a much lower reaction barrier at θ_H = 0.75 ML than at θ_H = 0.5 ML (0.20 eV vs 0.71 eV). We expect reaction-reversibility to be important and this is taken into account in the microkinetic modeling reported below.

Figure 6 compares the potential energy surfaces of furfural hydrogenation to furfuryl alcohol at θ_H = 0.5 ML, 0.75 ML, and

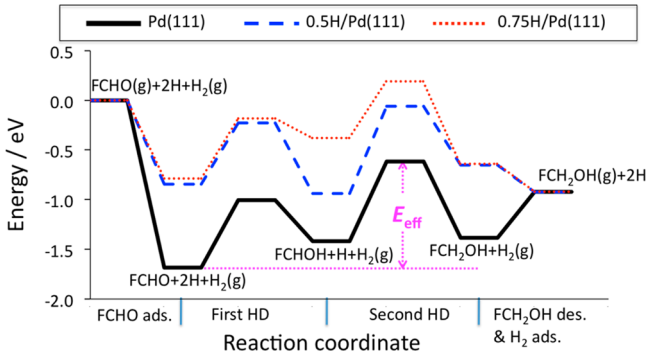

Figure 6. Energy profile of furfural hydrogenation to furfuryl alcohol at different coverages of H. The data on clean Pd(111) (black line) are taken from ref . Intermediates are taken in their most stable adsorbed conformation.

on bare Pd(111). On bare Pd(111), we report values without lateral interactions (the energies of adsorbates are calculated in separate slabs). For other coverages, the energies are calculated on hydrogen-covered surfaces to account for lateral interactions.

For the reaction coordinate in Figure 6, the reaction starts with the gas-phase furfural, H_2, and the coadsorbed hydrogen (in order to see the effect of adsorbed H). The steps in sequence include the adsorption of furfural on the surface, the addition of hydrogen to the oxygen of the −CHO group, and the addition of hydrogen to the carbon of the side group; the last step combines the desorption of furfuryl alcohol and the adsorption of H_2. We do not discuss these two steps in the paper any further and combine them to simplify the graph.

For hydrogenation on bare Pd(111), the adsorption of furfural is strong with an adsorption energy of −1.68 eV. The first and second hydrogenation steps are endothermic and thermoneutral (0.27 and 0.03 eV), respectively. It is clear that the potential energy drops largely due to furfural adsorption and increases in subsequent reactions. This indicates that bare Pd(111) binds too strongly and may hinder the desorption of products.

Based on the energy span theory,[41,42] the effective barrier (E_{eff}) of the hydrogenation of furfural is the energy difference between the transition state of the second hydrogenation step (highest energy state along the pathway) and the initial state of the first hydrogenation step (lowest energy state along the pathway), as shown in Figure 6. E_{eff} is 1.07 eV on bare Pd(111), 0.78 eV at θ_H = 0.5 ML, and 0.98 eV at θ_H = 0.75 ML. As a result, the energy span model shows that the effective barrier for hydrogenation of furfural to furfuryl alcohol should exhibit a minimum with increasing H coverage.

FURFURAL DECARBONYLATION

It has been proposed that the first and rate-determining step in decarbonylation of furfural is the dehydrogenation of the formyl group.[40] Upon hydrogen scission (formation of FCO), the molecule decomposes easily into F and CO.[15] Therefore, we calculated the energy barriers of the rate-determining step at

dx.doi.org/10.1021/cs5015145 | ACS Catal. 2015, 5, 104−112

θ_H = 0.5 and 0.75 ML. The structures and forward and backward energy barriers are shown in Figure 7. For the

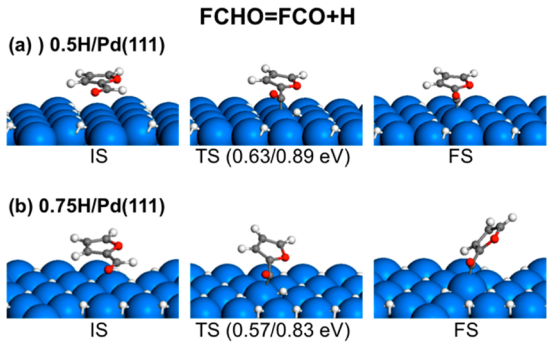

Figure 7. Structures of initial state (IS), transition state (TS), and final state (FS) in the first step of dehydrogenation of furfural at hydrogen coverage of 0.5 and 0.75 ML.

reactions after the rate-determining step, we estimated the barriers using BEP relations (Supporting Information, Figures S4 and S5) developed in our previous paper.[43] The potential energy surfaces are shown in Figure 8 together with that on

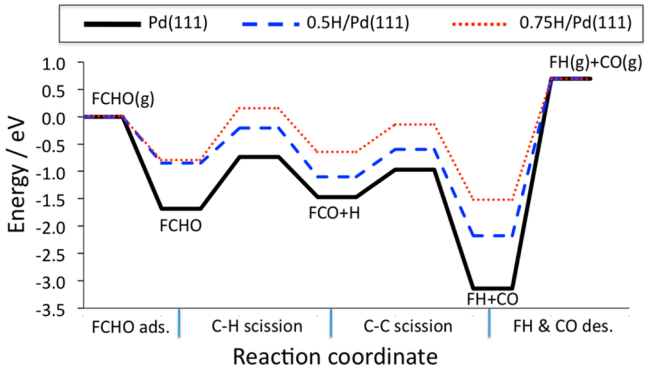

Figure 8. Energy profile of furfural decarbonylation at different hydrogen coverages. The data on clean Pd(111) (black line) are taken from ref 16.

bare Pd(111). The energy barrier of the rate-determining step on bare Pd(111), at θ_H = 0.5 and θ_H = 0.75 is 0.95, 0.63, and 0.94 eV, respectively. Analysis of energy barriers shows that the effective barrier of furfural decarbonylation should exhibit a minimum at intermediate hydrogen coverage.

It has been observed that the state of the Pd catalyst varies with conditions and the activity of hydrogen changes accordingly. For example, formation of hydride and a CO monolayer were thought to be responsible for the selectivity changes in the hydrogenation of an alkyne.[44] We expect similar effects on the selectivity of furfural chemistry studied here. Although we focus on the metallic Pd surface and the effect of hydrogen coverage on the conformation, the effect of additional catalyst states is an important topic for future work.

EFFECT OF OPERATING CONDITIONS ON ACTIVITY AND SELECTIVITY

We have investigated the hydrogenation and decarbonylation of furfural via microkinetic modeling by varying both temperature and pressure using the three DFT-parametrized models: low coverage, 0.5 ML of H, and 0.75 ML of H (Table 1). Calculations (Supporting Information, Figure S8) indicate that under experimentally relevant high pressure conditions investigated herein, the H coverage is high, and thus, in the remaining of the results, only the high coverage (0.75 ML H) parametrized model is used. However, it is quite possible that under other conditions and on other catalysts, one may be "switching" rate constants as operating conditions vary. Numerically, this can easily be done with a simple interpolation model to ensure continuity and smoothness. What is remarkable is that the hydrogenation and decarbonylation rates vary drastically up to 6 and 3 orders of magnitude, respectively, depending on the H coverage. Hydrogenation is more sensitive to the conformation change, and decarbonylation exhibits nonmonotonic dependence with varying H coverage. The low-H coverage model predicts only decarbonylation to furan with no furfuryl alcohol, whereas the higher H coverage models predict a transition from decarbonylation to hydrogenation as operating conditions change.

Under typical reactor conditions, the effect of hydrogen partial pressure at 190 °C is shown in Figure 9. H is the most abundant surface species. Specifically, the hydrogen coverage varies between 0.70 and 0.90 ML in this pressure regime, consistent with the DFT microkinetic model's parametrization. The coverages of furans and CO remain low under these conditions. The reaction rates increase with partial H_2 pressure and exhibit a maximum. This indicates that the overall rate may not benefit from very high pressures due to blocking of catalyst

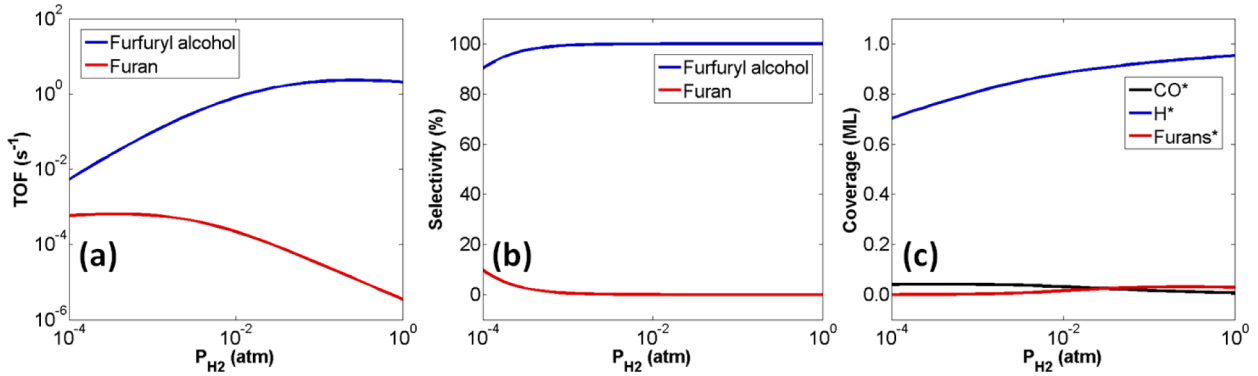

Figure 9. Microkinetic modeling results for initial (a) turnover frequency (TOF) to furfuryl alcohol, (b) selectivities, and (c) surface coverage vs hydrogen partial pressure at 190 °C using the high hydrogen coverage (0.75 ML) parametrized model. The furfural/H_2 molar ratio was kept at 1:25 in all simulations.

dx.doi.org/10.1021/cs5015145 | ACS Catal. 2015, 5, 104−112

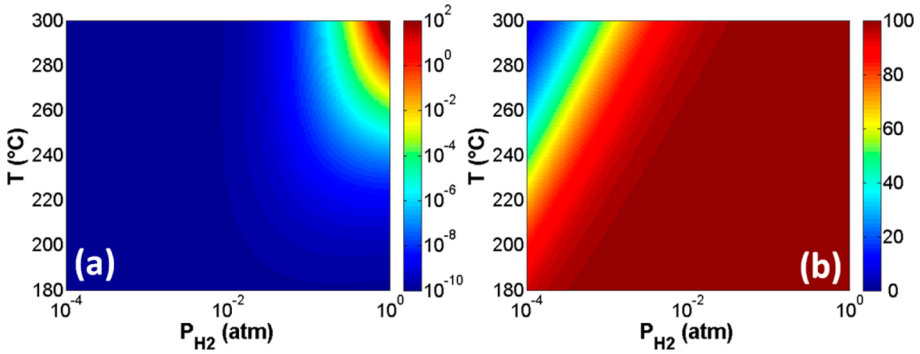

Figure 10. Initial furfuryl alcohol (a) turnover frequency (TOF) (s^{-1}) and (b) % selectivity vs hydrogen partial pressure and temperature using the high hydrogen coverage (0.75 ML) parametrized-model. The furfural/H_2 molar ratio was kept at 1:25 in all simulations.

sites by H. At this temperature, the hydrogenation selectivity is high compared to decarbonylation and is expected to be ~100% at most hydrogen partial pressures of interest.

Figure 10 shows the combined effect of temperature and hydrogen partial pressure on furfuryl alcohol activity and selectivity. The rate of furfuryl alcohol increases with both hydrogen partial pressure and temperature. The selectivity to furfuryl alcohol is higher at lower temperatures and higher hydrogen partial pressures and increases at fixed temperature with increasing H_2 pressure. Furan is favored at low H_2 pressures and with increasing temperature. The trend suggests that selectivity is mainly a function of hydrogen partial pressure as opposed to temperature. This is consistent with the experimental results of Resasco and co-workers, who showed a small decrease in hydrogenation selectivity with increasing temperature.[8,39]

Importantly, the low-coverage parametrized-model shows no selectivity toward hydrogenation to furfuryl alcohol in the considered temperature and pressure ranges (Figure S9); instead, decarbonylation occurs, converting furfural to furan. These findings suggest that only the high-coverage model is capable of correctly identifying the selectivity trends in qualitative agreement with experimental results.[7,8] In this regard, the conformation change with increasing H coverage induces a selectivity reversal from furan as the main product (low H coverage limit) to furfuryl alcohol (high H coverage limit). Our low-H coverage limit-model, which shows no selectivity to furfuryl alcohol, may provide an explanation for the findings of Pang and Medlin, who observed no hydrogenation of furfural over Pd(111) under ultrahigh vacuum (UHV) conditions.[14] H surface coverage could be low at UHV conditions, especially due to diffusion of H to the bulk of Pd and the lack of an external H_2 supply, which may make the low coverage model relevant at UHV conditions.

Garcia-Mota et al. studied the effect of catalyst state on the alkyne hydrogenation on Pd catalyst:[44] they found that a hydride improves the selectivity to alkane; a carbide improves the selectivity to alkene; and a CO layer on the surface preferentially inhibits oligomer formation due to the ensemble effect. While coverage effects have previously been shown to have an important effect on catalyst activity, to our knowledge, this is the first time where coverage-induced conformational change of one of the coreactants by the high coverage of the other is found to lead to selectivity reversal. Although the exact values where such conformational changes occur will obviously depend on catalyst and conditions, we propose that such behavior is generic for hydrodeoxygenation of furanics and potentially other multifunctional molecules. Thus, in order to promote hydrogenation of the −CHO group over decarbonylation, aside from tuning the catalyst so that tilted conformations are preferred, operating conditions could have a profound effect on selectivity.

CONCLUSIONS

The adsorption, hydrogenation, and decarbonylation of furfural on clean and hydrogen-covered Pd(111) was investigated using density functional theory (DFT). It was found that the adsorbed conformation of furfural is affected by its own coverage. At low coverage, furfural binds on Pd(111) flat via both the furan ring and its carbonyl group. At high coverages, a tilted conformation, with two carbon atoms of the furan ring binding to Pd(111), becomes the most stable. A similar trend was also observed for furfural adsorption on hydrogen covered Pd(111); furfural absorbs flat at low hydrogen coverages and tilted with its carbonyl group interacting with the surface at high hydrogen coverages.

Hydrogen adsorption on the surface profoundly changes the energy profile compared to that on a clean Pd(111) surface. The intermediates and transition states have higher energies than on clean Pd(111), resulting in a "shallower" potential energy surface. Based on the energy span model, the effective barrier for hydrogenation and decarbonylation is actually lowest at intermediate coverages of H. The selectivity to hydrogenation over decarbonylation increases with H coverage or hydrogen pressure and decreases with increasing temperature.

Microkinetic modeling was carried out using three sets of DFT calculated parameters. The conformation change with increasing H coverage induces a selectivity reversal from furan as the main product (low-H coverage limit) to furfuryl alcohol (high-H coverage limit). The selectivity of furfuryl alcohol is mainly a function of hydrogen partial pressure as opposed to temperature. Under typical hydrodeoxygenation reactor operating conditions, high coverages of H may be expected, leading to the tilted conformation of furfural and enhanced hydrogenation over decarbonylation. At UHV conditions, the H surface coverage could be low (in part due to diffusion to bulk Pd), leading to the flat furfural conformation and furfural decarbonylation rather than hydrogenation to furfuryl alcohol. Our results provide a rationale for the disparity in the selectivity seen experimentally over a wide range of hydrogen pressures. Importantly, this study underscores the potential importance of operating conditions on hydrodeoxygenation activity and selectivity due to conformational changes.

dx.doi.org/10.1021/cs5015145 | ACS Catal. 2015, 5, 104−112

■ ASSOCIATED CONTENT

Supporting Information

The following file is available free of charge on the ACS Publications website at DOI: 10.1021/cs5015145.

Adsorption structures of furfural on Pd(111) at low coverages (PDF)

■ AUTHOR INFORMATION

Corresponding Author

*E-mail: vlachos@udel.edu.

Notes

The authors declare no competing financial interest.

■ ACKNOWLEDGMENTS

We acknowledge support from the Catalysis Center for Energy Innovation, an Energy Frontier Research Center funded by the U.S. Department of Energy, Office of Science, Office of Basic Energy Sciences under Award No. DE-SC0001004. This research used resources of the National Energy Research Scientific Computing Center, a DOE Office of Science User Facility supported by the Office of Science of the U.S. Department of Energy under Contract No. DE-AC02-05CH11231.

■ REFERENCES

(1) Serrano-Ruiz, J. C.; West, R. M.; Dumesic, J. A. *Annu. Rev. Chem. Biomol. Eng.* **2010**, *1*, 79−100.
(2) Chang, C.-C.; Green, S. K.; Williams, C. L.; Dauenhauer, P. J.; Fan, W. *Green Chem.* **2014**, *16*, 585−588.
(3) Sitthisa, S.; An, W.; Resasco, D. E. *J. Catal.* **2011**, *284*, 90−101.
(4) Sitthisa, S.; Sooknoi, T.; Ma, Y.; Balbuena, P. B.; Resasco, D. E. *J. Catal.* **2011**, *277*, 1−13.
(5) Li, H.; Luo, H.; Zhuang, L.; Dai, W.; Qiao, M. *J. Mol. Catal. A* **2003**, *203*, 267−275.
(6) Liaw, B.; Chiang, S.; Chen, S.; Chen, Y. *Appl. Catal., A* **2008**, *346*, 179−188.
(7) Kijeński, J.; Winiarek, P.; Paryjczak, T.; Lewicki, A.; Mikołajska, A. *Appl. Catal., A* **2002**, *233*, 171−182.
(8) Sitthisa, S.; Resasco, D. E. *Catal. Lett.* **2011**, *141*, 784−791.
(9) Seo, G.; Chon, H. *J. Catal.* **1981**, *67*, 424−429.
(10) Rao, R.; Dandekar, A.; Baker, R. T. K.; Vannice, M. A. *J. Catal.* **1997**, *171*, 406−419.
(11) Reddy, B. M.; Reddy, G. K.; Rao, K. N.; Khan, A.; Ganesh, I. *J. Mol. Catal. A* **2007**, *265*, 276−282.
(12) Liu, B.; Cheng, L.; Curtiss, L.; Greeley, J. *Surf. Sci.* **2014**, *622*, 51−59.
(13) Medlin, J. W. *ACS Catal.* **2011**, *1*, 1284−1297.
(14) Yu, W.; Xiong, K.; Ji, N.; Porosoff, M. D.; Chen, J. G. *J. Catal.* **2014**, *317*, 253−262.
(15) Vorotnikov, V.; Mpourmpakis, G.; Vlachos, D. G. *ACS Catal.* **2012**, *2*, 2496−2504.
(16) Wang, S.; Vorotnikov, V.; Vlachos, D. G. *Green Chem.* **2014**, *16*, 736−747.
(17) Pang, S. H.; Schoenbaum, C. A.; Schwartz, D. K.; Medlin, J. W. *Nat. Commun.* **2013**, *4*, 2448.
(18) Marshall, S. T.; Medlin, J. W. *Surf. Sci. Reports* **2011**, *66*, 173−184.
(19) Grabow, L. C.; Hvolbæk, B.; Nørskov, J. K. *Top. Catal.* **2010**, *53*, 298−310.
(20) Xu, Y.; Lausche, A. C.; Wang, S.; Khan, T. S.; Abild-Pedersen, F.; Studt, F.; Nørskov, J. K.; Bligaard, T. *New J. Phys.* **2013**, *15*, 125021.
(21) Park, Y. K.; Aghalayam, P.; Vlachos, D. G. *J. Phys. Chem. A* **1999**, *103*, 8101−8107.
(22) Mhadeshwar, A. B.; Kitchin, J. R.; Barteau, M. A.; Vlachos, D. G. *Catal. Lett.* **2004**, *96*, 13−22.
(23) Ulissi, Z.; Prasad, V.; Vlachos, D. G. *J. Catal.* **2011**, *281*, 339−344.
(24) Griffin, M. B.; Pang, S. H.; Medlin, J. W. *J. Phys. Chem. C* **2012**, *116*, 4201−4208.
(25) Kresse, G.; Furthmuller, J. *Comput. Mater. Sci.* **1996**, *6*, 15−50.
(26) Kresse, G.; Furthmuller, J. *Phys. Rev. B* **1996**, *54*, 11169.
(27) Perdew, J. P.; Burke, K.; Ernzerhof, M. *Phys. Rev. Lett.* **1996**, *77*, 3865.
(28) Grimme, S.; Antony, J.; Ehrlich, S.; Krieg, H. *J. Chem. Phys.* **2010**, *132*, 154104.
(29) Blochl, P. E. *Phys. Rev. B* **1994**, *50*, 17953.
(30) Kresse, G.; Joubert, D. *Phys. Rev. B* **1999**, *59*, 1758.
(31) Monkhorst, H. J.; Pack, J. D. *Phys. Rev. B* **1976**, *13*, 5188.
(32) Blochl, P. E.; Jepsen, O.; Andersen, O. K. *Phys. Rev. B* **1994**, *49*, 16223.
(33) Lamber, R.; Wetjen, S.; Jaeger, N. I. *Phys. Rev. B* **1995**, *51*, 10968.
(34) Henkelman, G.; Uberuaga, B. P.; Jonsson, H. *J. Chem. Phys.* **2000**, *113*, 9901.
(35) Salciccioli, M.; Stamatakis, M.; Caratzoulas, S.; Vlachos, D. G. *Chem. Eng. Sci.* **2011**, *66*, 4319−4355.
(36) Vorotnikov, V.; Wang, S.; Vlachos, D. G. *Ind. Eng. Chem. Res.* **2014**, *53*, 11929−11938.
(37) Sutton, J. E.; Panagiotopoulou, P.; Verykios, X. E.; Vlachos, D. G. *J. Phys. Chem. C* **2013**, *117*, 4691−4706.
(38) Salciccioli, M.; Vlachos, D. G. *ACS Catal.* **2011**, *1*, 1246−1256.
(39) Sitthisa, S.; Pham, T.; Prasomsri, T.; Sooknoi, T.; Mallinson, R. G.; Resasco, D. E. *J. Catal.* **2011**, *280*, 17−27.
(40) van Druten, G. M. R.; Ponec, V. *Appl. Catal. A: Gen.* **2000**, *191*, 163−176.
(41) Kozuch, S. *WIREs Comput. Mol. Sci.* **2012**, *2*, 795−815.
(42) Kozuch, S.; Shaik, S. *Acc. Chem. Res.* **2011**, *44*, 101−110.
(43) Wang, S.; Vorotnikov, V.; Sutton, J. E.; Vlachos, D. G. *ACS Catal.* **2014**, *4*, 604−612.
(44) Garcia-Mota, M.; Bridier, B.; Perez-Ramirez, J.; Lopez, N. *J. Catal.* **2010**, *273*, 92−102.